Bacterial formate hydrogenlyase complex

Jennifer S. McDowall[a,1,2], Bonnie J. Murphy[b,1], Michael Haumann[c], Tracy Palmer[a], Fraser A. Armstrong[b], and Frank Sargent[a,3]

[a]Division of Molecular Microbiology, College of Life Sciences, University of Dundee, Dundee DD1 5EH, Scotland; [b]Inorganic Chemistry Laboratory, Department of Chemistry, University of Oxford, Oxford OX1 3QR, United Kingdom; and [c]Institut für Experimentalphysik, Freie Universität Berlin, 14195 Berlin, Germany

Edited by Lonnie O. Ingram, University of Florida, Gainesville, FL, and approved July 25, 2014 (received for review April 30, 2014)

Under anaerobic conditions, *Escherichia coli* can carry out a mixed-acid fermentation that ultimately produces molecular hydrogen. The enzyme directly responsible for hydrogen production is the membrane-bound formate hydrogenlyase (FHL) complex, which links formate oxidation to proton reduction and has evolutionary links to Complex I, the NADH:quinone oxidoreductase. Although the genetics, maturation, and some biochemistry of FHL are understood, the protein complex has never been isolated in an intact form to allow biochemical analysis. In this work, genetic tools are reported that allow the facile isolation of FHL in a single chromatographic step. The core complex is shown to comprise HycE (a [NiFe] hydrogenase component termed Hyd-3), FdhF (the molybdenum-dependent formate dehydrogenase-H), and three iron-sulfur proteins: HycB, HycF, and HycG. A proportion of this core complex remains associated with HycC and HycD, which are polytopic integral membrane proteins believed to anchor the core complex to the cytoplasmic side of the membrane. As isolated, the FHL complex retains formate hydrogenlyase activity in vitro. Protein film electrochemistry experiments on Hyd-3 demonstrate that it has a unique ability among [NiFe] hydrogenases to catalyze production of H_2 even at high partial pressures of H_2. Understanding and harnessing the activity of the FHL complex is critical to advancing future biohydrogen research efforts.

bacterial hydrogen metabolism | PFE

The Gram-negative facultative anaerobe *Escherichia coli* is a member of the γ-Proteobacteria, a group of bacteria that are renowned for their metabolic flexibility (1). During anaerobic fermentative growth (i.e., in the absence of all exogenous electron acceptors), *E. coli* performs a mixed-acid fermentation, using glucose as the sole carbon and energy source and producing formate, succinate, acetate, lactate, and ethanol as products. When extracellular formate levels reach a critical threshold, with a concomitant drop in environmental pH, the formate is transported back into the cell cytoplasm via a specific transporter where the membrane-bound formate hydrogenlyase (FHL) complex disproportionates formate, producing CO_2 and H_2 (2). The standard (pH-corrected) thermodynamic driving force for this reaction is small, but the volatility of the products helps to drive the continued oxidation of formate under physiological conditions (3, 4). The FHL complex is responsible for the vast majority of molecular hydrogen evolved during glucose fermentation by enteric bacteria (5, 6); thus, understanding and harnessing this activity is important if the full potential of biologically produced hydrogen ("biohydrogen") is to be realized.

The ability of *E. coli* to evolve hydrogen by decomposition of formate was first described over 100 years ago by Pakes and Jollyman (7). Since then, over 100 papers have been published on this reaction, including seminal studies on the physiology and biochemistry (8, 9), expression, and maturation (5, 10–14), as well as the potential for biohydrogen applications (6, 15). Despite this, the *E. coli* FHL complex has never been isolated in an intact or active state.

The formate dehydrogenase reaction

$$HCOO^- \rightarrow CO_2 + H^+ + 2e^- \ (E_0' = +432 \ \text{mV}\,[16])$$

of FHL is carried out by a molybdenum-dependent selenoenzyme (encoded by the *fdhF* gene), which has been studied in detail by X-ray crystallography (12, 17), X-ray absorption spectroscopy (18), and electron paramagnetic resonance (EPR) spectroscopy (19, 20). Electrons derived from formate oxidation are used for the reduction of protons to dihydrogen at the [NiFe] hydrogenase catalytic subunit, HycE (5, 10):

$$2H^+ + 2e^- \rightarrow H_2 \ (E_0' = -414 \ \text{mV}\,[16]).$$

The thermodynamic potentials for the half-cell reactions apply for pH 7, and partial gas pressures $\rho(CO_2)$ and $\rho(H_2)$ each at 1 atmosphere: The resulting 18-mV driving force must be adjusted upward to reflect the fact that it increases by 30 mV for each decade decrease in $\rho(CO_2)$ and $\rho(H_2)$ as well as by 30 mV for each decrease in pH unit.

[NiFe] hydrogenases are widespread in prokaryotes and consist minimally of a catalytic α-subunit of ∼60 kDa, which houses an elaborate Ni–Fe(CO)$(CN)_2$ cofactor, and an electron transferring β-subunit (∼35 kDa) containing between one and three Fe–S clusters (21, 22). In FHL, the α-subunit (HycE) is predicted to partner with HycG, and together they comprise the minimal catalytic unit of *E. coli* hydrogenase-3 (Hyd-3) (11). *E. coli* Hyd-3 is unusual among well-characterized [NiFe] hydrogenases in that most are involved predominantly in respiratory H_2 oxidation (23), whereas Hyd-3 is predominantly involved in H_2 production, as is common for the "Group 4" [NiFe] hydrogenases (24) to which HycE belongs. HycE is predicted to contain two separate domains, with the C-terminal residues 172–539 encoding the typical [NiFe] hydrogenase and the N-terminal residues 1–166 encoding

Significance

The isolation of an active formate hydrogenlyase is a breakthrough in understanding the molecular basis of bacterial hydrogen production. For over 100 years, *Escherichia coli* has been known to evolve H_2 when cultured under fermentative conditions. Glucose is metabolized to formate, which is then oxidized to CO_2 with the concomitant reduction of protons to H_2 by a single complex called formate hydrogenlyase, which had been genetically, but never biochemically, characterized. In this study, innovative molecular biology and electrochemical experiments reveal a hydrogenase enzyme with the unique ability to sustain H_2 production even under high partial pressures of H_2. Harnessing bacterial H_2 production offers the prospect of a source of fully renewable H_2 energy, freed from any dependence on fossil fuel.

Author contributions: J.S.M., B.J.M., F.A.A., and F.S. designed research; J.S.M., B.J.M., M.H., T.P., and F.S. performed research; J.S.M., B.J.M., M.H., T.P., F.A.A., and F.S. analyzed data; and J.S.M., B.J.M., M.H., T.P., F.A.A., and F.S. wrote the paper.

The authors declare no conflict of interest.

This article is a PNAS Direct Submission.

Freely available online through the PNAS open access option.

[1]J.S.M. and B.J.M. contributed equally to this work.

[2]Present address: Department of Biology and Biochemistry, University of Bath, Bath BA2 7AY, United Kingdom.

[3]To whom correspondence should be addressed. Email: f.sargent@dundee.ac.uk.

This article contains supporting information online at www.pnas.org/lookup/suppl/doi:10.1073/pnas.1407927111/-/DCSupplemental.

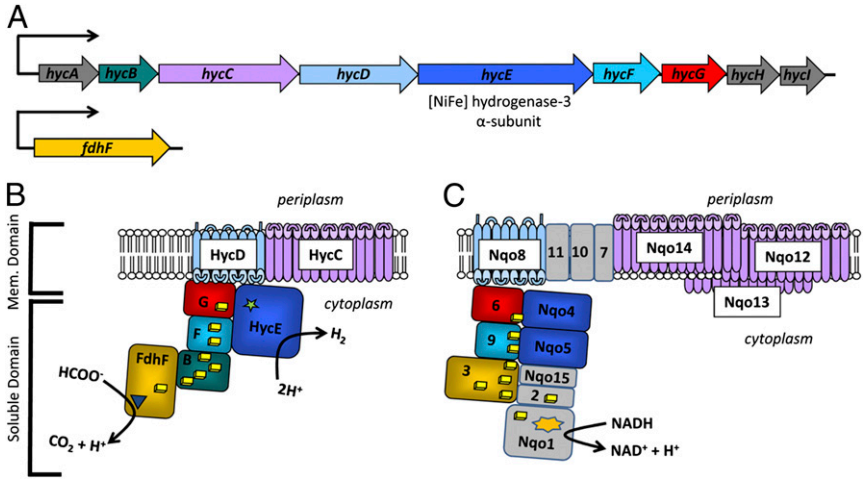

Fig. 1. The genetics and predicted structure of formate hydrogenlyase. (*A*) The genetic organization of the *E. coli hycABCDEFGHI* operon and the *fdhF* gene. Genes colored gray do not encode components of the final enzyme. The gene encoding the catalytic subunit of Hyd-3 is indicated. (*B*) Predicted architecture of the *E. coli* FHL complex. Proteins are color-coded corresponding to their respective genes from *A*. (*C*) Cartoon of *E. coli* Complex I color-coded to highlight similarity with FHL.

an apparently cofactorless polypeptide with homology to NuoC/Nqo5 proteins from Complex I (Fig. 1). Genetic and computational analysis (4, 11) suggests that the remainder of the complex consists of a series of Fe–S proteins that mediate electron transfer from the formate dehydrogenase to the core Hyd-3 moiety. HycB is predicted to contain four [4Fe–4S] clusters and interact directly with FdhF, whereas HycF is predicted to contain at least two [4Fe–4S] clusters and models place it between HycB and the Hyd-3 β-subunit HycG, which itself is predicted to contain one [4Fe–4S] cluster (Fig. 1). With the exception of the *fdhF* gene encoding the formate dehydrogenase, all of the predicted components of FHL are encoded by the *hycABCDEFGHI* operon (Fig. 1*A*) (10, 13). As well as the structural subunits, the *hyc* operon encodes a transcriptional repressor (HycA) (11) and two proteins involved in the biosynthesis of Hyd-3 (HycH and HycI) (13).

FHL activity can be readily assayed in whole cells, and bidirectional Hyd-3 activity can be measured in crude extracts using a redox dye as the electron acceptor or donor (5). However, isolation of the intact FHL complex has never been reported due to its extreme lability (5, 25). In this work, genetic engineering approaches have been used to allow the rapid isolation of the intact FHL complex. The enzyme has been purified in a single step and is shown to contain all of the predicted subunits as well as exhibiting FHL activity in vitro. Protein film electrochemistry (PFE) experiments show that Hyd-3 is unique among [NiFe] hydrogenases characterized to date, in that H_2 production is only very weakly product inhibited, with an inhibition constant comparable to values measured for [FeFe] hydrogenases, an evolutionarily distinct class of hydrogenases usually dedicated to H_2 production and not found in *E. coli* (21). Despite this, the $K_M^{H_2}$ for hydrogen oxidation is not comparable to the relatively high values for [FeFe] hydrogenases but is instead in the range of other [NiFe] hydrogenase enzymes.

Results

Affinity Tagging of Fe–S Subunits of the FHL Complex. The initial aim of this work was to characterize components of the FHL complex at physiologically relevant levels of expression. The FHL complex is predicted to contain three electron-transferring Fe–S proteins termed HycB, HycF, and HycG. Sequence analysis suggests HycG is the most likely candidate for the Hyd-3 β-subunit (11), although this has never been proven experimentally. Three strains were constructed in the MG1655 wild-type *E. coli* K-12 genetic background incorporating hexahistidine tags at the C terminus of each designated gene product (Table 1). The new strains, MG059b ($hycB^{His}$), MG059f ($hycF^{His}$), and MG059g ($hycG^{His}$), were carefully constructed to preserve initiation codons and ribosome binding sites of any downstream genes.

The physiological hydrogen evolution activity of each of the mutant strains was assessed directly. In each case, formate-dependent H_2 evolution rates for intact cells cultured under fermentative conditions were comparable to that of the parent strain (Fig. 2*A*). The addition of C-terminal affinity tags to the HycB, HycF, or HycG proteins results in strains with unimpaired physiological activity of the FHL complex, because eliminating FHL activity in *E. coli* leads to a strain with minimal-to-no H_2 production activity under these growth and assay conditions (11). Next, the hexahistidine tags were exploited to assess the subcellular localizations of the engineered Fe–S proteins. Cells of each strain were grown under anaerobic fermentative conditions, harvested, and separated into soluble and membrane-associated protein fractions (Fig. 2*B*). Subsequent Western analysis revealed $HycB^{His}$, $HycF^{His}$, and $HycG^{His}$ to be associated with the membrane fraction (Fig. 2*B*), consistent with the predicted localization of the FHL complex.

Affinity Tagging of the [NiFe] Hydrogenase Subunit of the FHL Complex. To study the catalytic [NiFe] hydrogenase subunit (HycE) itself, a strategy was devised for the affinity tagging of this protein. Because the HycE protein undergoes C-terminal cleavage during incorporation of the [NiFe] cofactor (25), the use of C-terminal affinity tags is not appropriate. Instead, a multiple sequence alignment of HycE-type proteins was used to identify regions of plasticity within the primary structure that might represent nonessential or surface-exposed regions. The HycE protein

Table 1. ***Escherichia coli*** **strains studied and constructed in this work**

Strain	Relevant genotype	Source
MG1655	*E. coli* K-12, F^-, λ^-, *ilvG*, *rfb-50*, *rph-1*	(42)
MG059b	as MG1655, $hycB^{His}$ (C-terminal His-tag)	this work
MG059e1	as MG1655, $hycE^{His}$ (internal His-tag)	this work
MG059f	as MG1655, $hycF^{His}$ (C-terminal His-tag)	this work
MG059g	as MG1655, $hycG^{His}$ (C-terminal His-tag)	this work

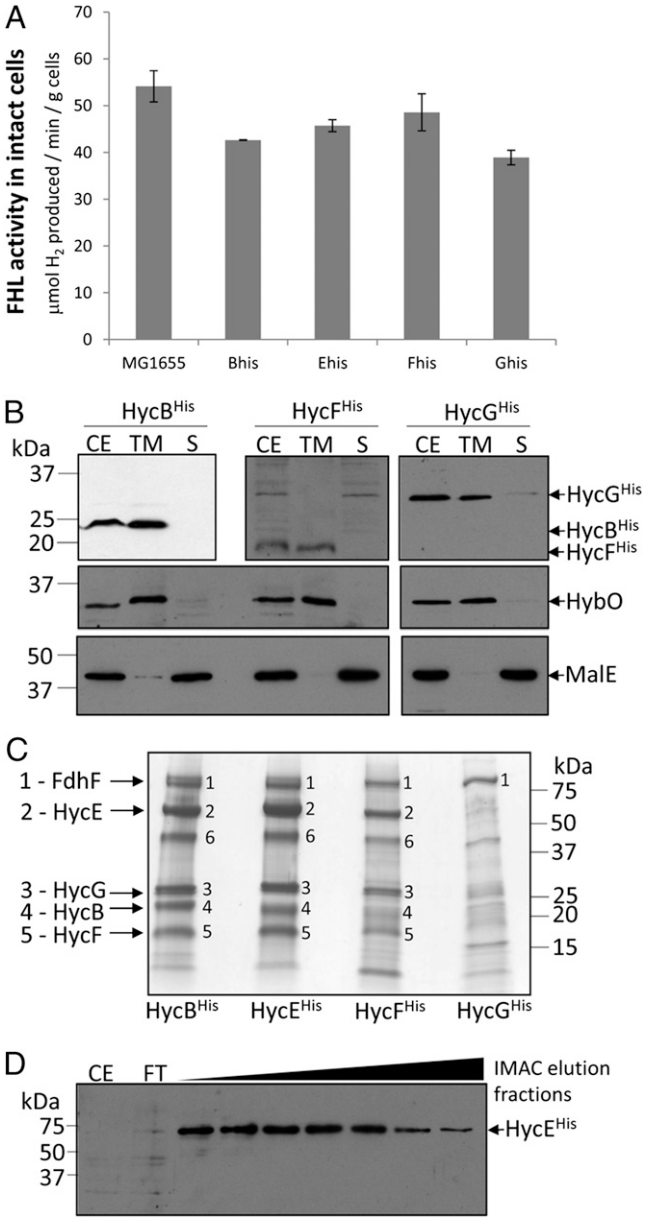

Fig. 2. Affinity tagging of formate hydrogenlyase components. (*A*) The affinity tags do not interfere with FHL activity. The parental strain (MG1655) and derivatives expressing *hycB*^{His} (Bhis), *hycE*^{His} (Ehis), *hycF*^{His} (Fhis), and *hycG*^{His} (Ghis) were grown anaerobically in LB media (pH 6.4) supplemented with 0.4% (wt/vol) glucose. Cells were harvested by centrifugation, washed twice in 50 mM Tris·HCl (pH 7.4), and intact cells then assayed for formate-dependent H_2 evolution in a H_2-sensing electrode as described (5, 47). Error bars represent the SEM, $n = 3$. (*B*) FHL Fe–S subunits remain membrane bound following cell lysis. Strains were grown under fermentative conditions before being harvested, washed, and fractionated in the absence of detergent. Equal proportions of crude extracts (CE), total membranes (TM), and soluble proteins (S) were separated by SDS-PAGE and challenged with an anti-His monoclonal antibody (*Upper*). Fractionation and loading control immunoblots toward the HybO integral membrane protein (*Middle*), and the soluble maltose binding protein (MalE, *Lower*) are included. (*C*) FHL can be isolated in a single step. Strains were lysed in a detergent mixture before extracts were applied to IMAC columns and bound proteins eluted and pooled. Approximately 10 μg of concentrated samples were separated by SDS-PAGE and stained with Instant Blue. All protein bands analyzed by tryptic peptide mass spectrometry are labeled: 1, positively identified as FdhF; 2, HycE; 3, HycG; 4, HycB; 5, HycF; and 6, predominantly fragments of HycE. (*D*) Isolated $HycE^{His}$ can be identified by Western immunoblotting. A CE of MG059e1 (*hycE*^{His}) was prepared from a detergent mixture (6 g of cells in 40 mL solution) and applied to a 5-mL IMAC column. The unbound protein (column flow-through, FT) was collected in 40 mL total. Bound proteins were eluted in a 30-mL gradient of 50–1,000 mM imidazole, and 10 × 1 mL peak fractions were collected, seven of which were applied to 12% (wt/vol) SDS-PAGE. Separated proteins were transferred to nitrocellulose and challenged with an anti-His monoclonal antibody.

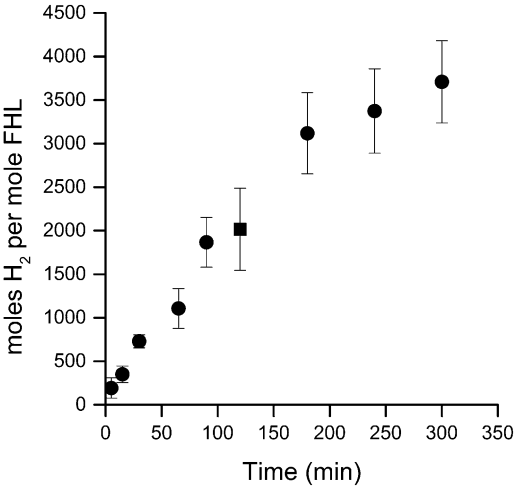

Fig. 3. FHL activity of the isolated FHL complex assayed in vitro. FHL was isolated for strain MG059e1 (*hycE*^{His}), suspended in 100 mM Mes pH 6.0, and incubated under N_2 with 2% CH_4 as calibrant gas for gas chromatography. Potassium formate solution (pH 6.5) was added to 50 mM (final concentration), and the reaction was allowed to proceed at 25 °C. H_2 concentration in the headspace was determined by gas chromatography. Error bars represent SE where $n = 3$, except for the data point at 120 min, where $n = 2$.

is predicted to comprise two domains: a cofactorless N-terminal domain, from amino acids 1–166, which shares homology with the 30-kDa subunit of NADH dehydrogenase (4), and a C-terminal domain, comprising amino acids 172–539, containing conserved motifs for binding the [NiFe] cofactor. This approach identified two possible regions of HycE that might accommodate an internal affinity tag: around the Gly-83 region or at the putative domain junction surrounding Thr-167. Two plasmids were designed and constructed, one encoding an internal stretch of 10 histidine residues between Gly-83 and Thr-84 and one encoding an identical tag between Glu-166 and Thr-167, of the HycE polypeptide. Only the allele encoding the insertion at Gly-83 was amenable to transfer to the chromosome. The resultant $HycE^{His}$ strain, MG059e1 (as MG1655, *hycE*^{His}), was shown to retain physiological formate-dependent H_2 production under fermentative growth conditions (Fig. 2*A*); however, it was not possible to reliably detect $HycE^{His}$ by Western immunoblotting in whole-cell extracts.

Isolation of Affinity-Tagged FHL Complexes Produced at Native Levels. *E. coli* strains MG059b, MG059e1, MG059f, and MG059g encoding $HycB^{His}$, $HycE^{His}$, $HycF^{His}$, and $HycG^{His}$, respectively, were grown under anaerobic, fermentative conditions. The harvested cells were lysed and membrane-bound components were solubilized in a single step using a detergent-containing chemical mixture. The crude lysate was applied directly to an immobilized metal affinity chromatography (IMAC) column, and, after extensive washing with buffer containing n-dodecyl-β-D-maltoside (DDM) detergent, bound proteins were eluted with a 0–1 M imidazole gradient and fractions were analyzed by SDS-PAGE (Fig. 2*C*). The stringent conditions used (50 mM imidazole in the sample and loading buffers, 200 mM NaCl and detergent throughout),

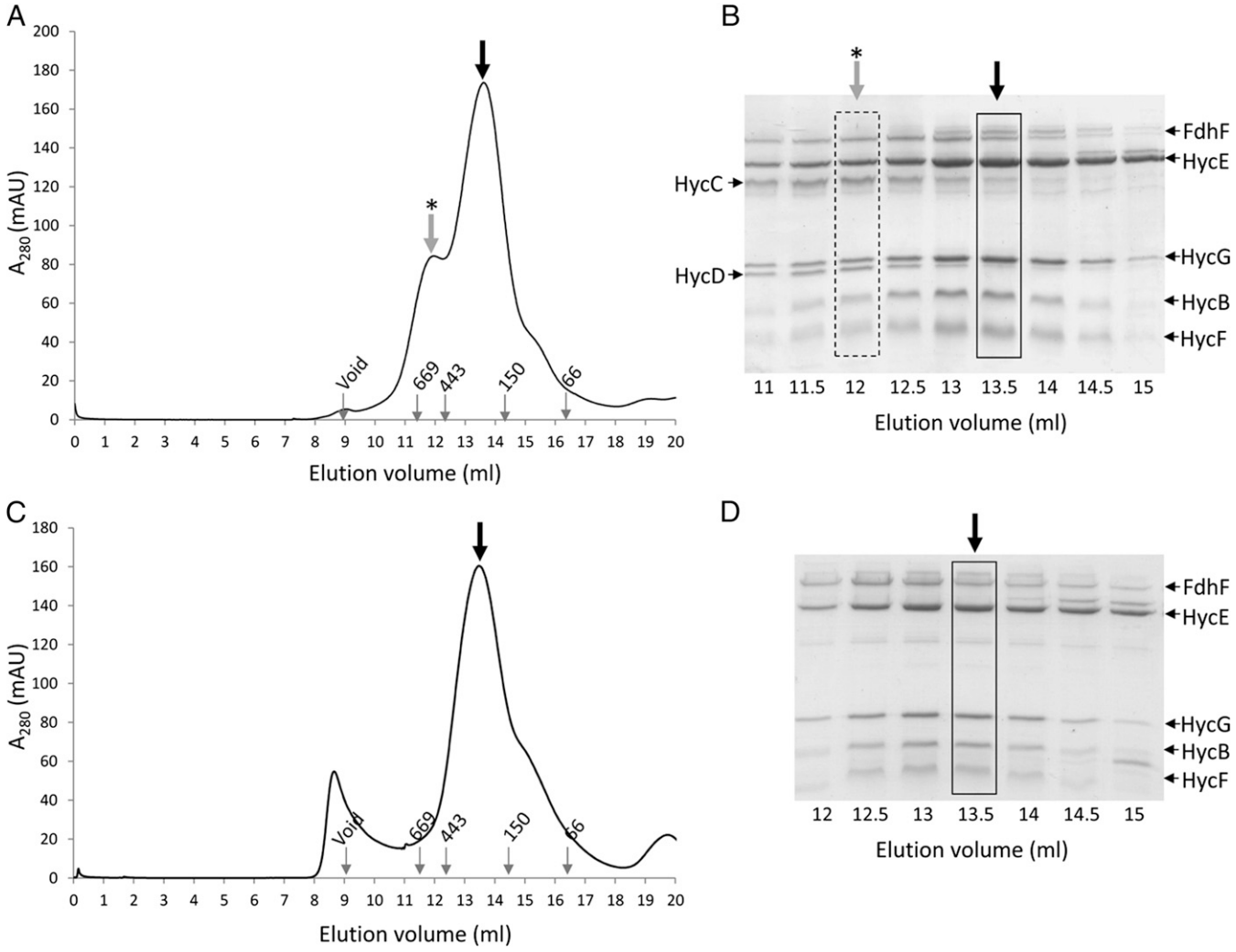

Fig. 4. Size-exclusion chromatography of the HycE^{His}-containing FHL complex. (*A*) Elution profile of HycE^{His} associated protein in the presence of detergent. The MG059e1 strain was lysed in a detergent mixture and applied to IMAC columns, and bound proteins were eluted and pooled in buffers containing 0.05% (wt/vol) DDM. Approximately 500 μg of pooled protein was then separated by SEC in buffers containing DDM. Fractions were separated by SDS-PAGE and stained with Instant Blue. (*B*) The peak fraction containing HycC and HycD is indicated by the asterisk. (*C*) Elution profile of HycE^{His} associated proteins in the absence of detergent. The strain was lysed in a detergent mixture and subjected to IMAC in the absence of all detergent. Approximately 500 μg of pooled protein was then separated by SEC in buffers devoid of detergent. Fractions were analyzed by SDS-PAGE (*D*). Proteins were identified by mass spectrometry and direct sequencing.

reduce nonspecific binding of native histidine-rich proteins to a minimum level (Fig. S1).

Using this protocol for the MG059e1 (*hycE*^{His}) strain, the [NiFe] hydrogenase subunit, HycE^{His}, was eluted from the IMAC column together with at least four other proteins (Fig. 2*C*), which were all identified by tryptic peptide mass fingerprinting. The protein migrating at ∼80 kDa was identified as FdhF (formate dehydrogenase H), while that migrating at ∼60 kDa was HycE itself; the bands around 30 kDa, 25 kDa, and 20 kDa were identified as HycG, HycB, and HycF, respectively (Fig. 2*C*). The prominent band migrating at ∼40 kDa was a proteolytic fragment of HycE, and analysis also revealed two peptide masses that could be attributed to fragments of HycC. Thus, internal affinity tagging of the [NiFe] hydrogenase subunit alone was sufficient to isolate at least five of the predicted FHL components in a single chromatographic step. Determination of ion content by total reflection X-ray fluorescence (TXRF) spectroscopy established that for every mole of nickel in the sample, there were ∼31 moles of iron, and substoichiometric but equivalent levels of both Se and Mo (∼0.3 moles). Metal analysis by inductively coupled plasma mass spectrometry (ICP-MS) produced similar data, where for every mole of ^{60}Ni present, another 37 moles of ^{56}Fe were detected together with 0.27 moles of ^{90}Mo. Given that the single molybdenum- and selenium-containing FdhF subunit is known to be only loosely attached to the complex, these ratios are consistent with the expected theoretical values (1 Ni: 1 Mo: 1 Se−Cys: 33 Fe). Although Western immunoblotting could not identify HycE^{His} in crude cell extracts, upon isolation by IMAC, the purified protein was readily detectable using anti-His monoclonal antibodies (Fig. 2*D*).

Importantly, the HycE^{His}-isolated complex retained formate hydrogenlyase activity in vitro (Fig. 3), with a maximum turnover rate, observed during the 90 min following addition of formate, of 20 min^{-1} (25 °C, 50 mM formate added initially). Although this in vitro rate is low, this is, to our knowledge, the first demonstration of the isolation of an active, intact formate hydrogenlyase enzyme complex.

For protein purified from the *hycB*^{His} strain MG059b, HycB^{His} coeluted with FdhF, HycG, HycE, and HycF (Fig. 2*C*), and all of these proteins were positively identified by mass spectrometry.

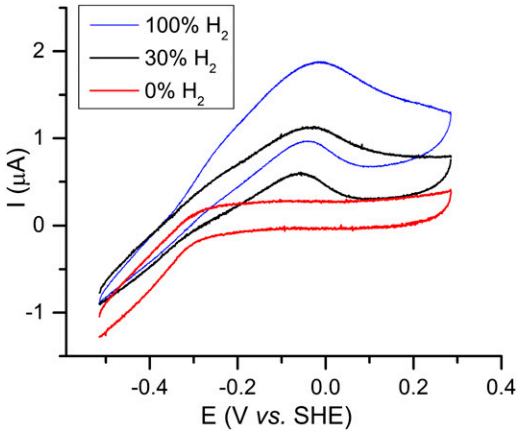

Fig. 5. Protein film voltammetry study of Hyd-3. Cyclic voltammograms were carried out at pH 6.0 (37 °C) under different amounts of H_2 as indicated. Nitrogen was used as the carrier gas, and the gas flow rate was 300 standard cubic centimeters per min (sccm). The electrode potential was increased from −0.56 to +0.24 V vs. SHE and then reversed, with a scan rate of 1 mV/s. Electrode rotation rate was 1,000 rpm.

Similarly, for the MG059f (*hycF*^{His}) strain, HycF^{His} protein coeluted with FdhF, HycB, HycE, and HycG (Fig. 2*C*), with each protein being identified by mass spectrometry. The addition of the hexahistidine tag to HycF affected its apparent electrophoretic mobility, and perhaps also the overall stability of the protein (Fig. 2 *B* and *C*).

For the MG059g (*hycG*^{His}) strain, although a normal level of H_2 production was observed (Fig. 2*A*) and the protein could be detected by immunoblotting (Fig. 2*B*), the complex was unstable to purification (Fig. 2*C*). The HycG^{His} protein coeluted from the IMAC column together with detectable amounts of the FdhF subunit (which was identified by mass spectrometry), but only trace amounts of other FHL components appeared to be present, together with a large degree of fragmentation or contamination (Fig. 2*C*). This strain was not studied further here.

Identification of the Integral Membrane Subunits HycC and HycD. The FHL complex isolated from the HycE^{His}-producing strain by IMAC was concentrated and loaded onto a Superose 6 Size Exclusion (SEC) column (Fig. 4*A*). The protein eluted as a main peak of ∼250 kDa, which was preceded by a shoulder containing higher-molecular-weight material (Fig. 4*A*). Analysis of the eluted fractions by SDS-PAGE revealed that the main 250-kDa peak contained FdhF, HycE^{His}, HycB, HycF, and HycG (Fig. 4*B*). These five proteins therefore represent the FHL "core complex" components that associate stably through two chromatographic steps. The preceding higher-molecular-weight shoulder also contained these five proteins (Fig. 4*B*), as well as a protein band at ∼30 kDa and a diffuse band at ∼45 kDa (Fig. 4*B*). Edman sequencing of the ∼45-kDa protein gave the sequence Met–Ser–Ala–Ile–Ser, corresponding exactly to the predicted N terminus of the HycC protein. Following Edman degradation analysis of the excised

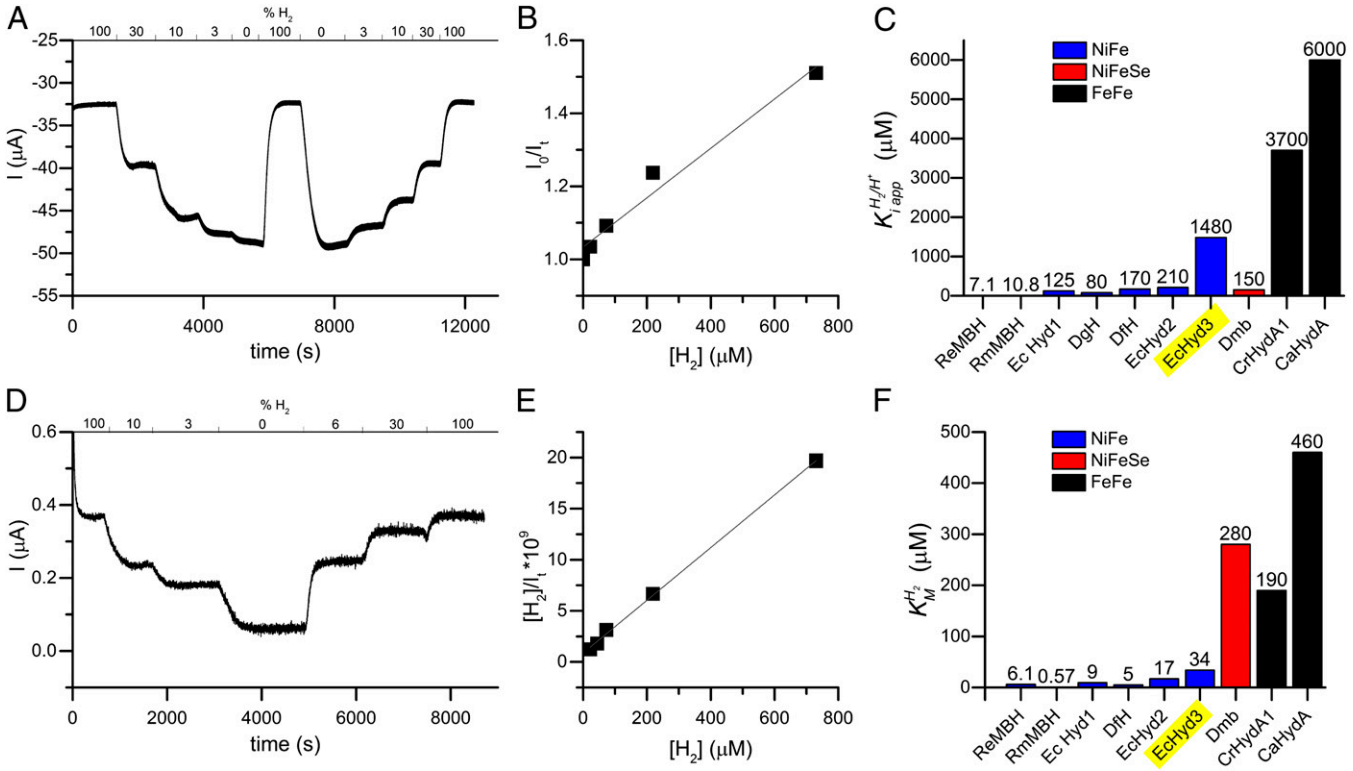

Fig. 6. Chronoamperometric determination of (*A* and *B*) the product inhibition ($K_i^{H_2/H^+}$) constant during proton reduction at −0.558 V vs. SHE and (*D* and *E*) the Michaelis–Menten ($K_M^{H_2}$) constant during H_2 oxidation at −0.108 V vs. SHE. Both experiments were carried out at pH 6.0, 37 °C, rotation rate 1,000 rpm, gas flow 1,000 sccm. Film loss was estimated according to the steady-state slope at each H_2 concentration, and data were corrected accordingly. (*C*) A comparison of $K_i^{H_2}$ values previously reported for various hydrogenase enzymes. (*F*) A comparison of $K_M^{H_2}$ values previously reported for various hydrogenase enzymes. Conditions for each measurement vary and are detailed in Table S1. ReMBH, *Ralstonia eutropha* membrane-bound hydrogenase (MBH); RmMBH, *R. metallidurans* MBH; Ec Hyd1, *E. coli* Hyd-1 (MBH); DgH, *Desulfovibrio gigas* hydrogenase; DfH, *D. fructosovorans* hydrogenase; Ec Hyd-1, *E. coli* Hyd-2 (MBH); EcHyd3, *E. coli* Hyd-3; Dmb, *Desulfomicrobium baculatum* [NiFeSe] hydrogenase; CrHydA1, *Chlamydomonas reinhardtii* HydA1; CaHydA, *Clostridium acetobutylicum* HydA.

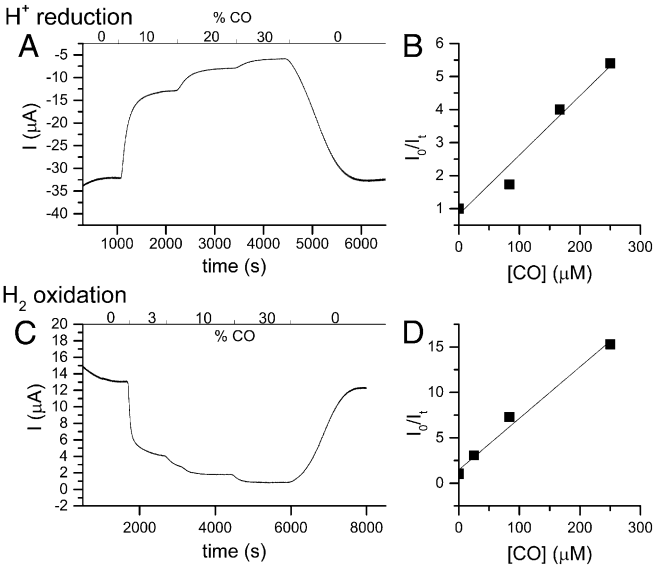

Fig. 7. Chronoamperometry experiments designed to assess the K_i^{CO} for Hyd-3 during H^+ reduction (*A* and *B*) and H_2 oxidation (*C* and *D*). Experimental conditions were as follows: pH 6.0, 37 °C, rotation rate 1,000 rpm, gas flow 300 sccm, 100% Ar (*A*) or 10% H_2 in Ar (*C*), −0.537 V vs. SHE (*A*), −0.087 V vs. SHE (*C*). K_i^{CO} values were 56 ± 17 μM for H^+ reduction (*B*) and 8.2 ± 1.8 μM for H_2 oxidation (*D*). Film loss was estimated according to the steady-state slope at each CO concentration, and data were corrected accordingly.

~30-kDa protein band, a sequence Met–Ile–Val–Leu–Tyr (where the methionine was partly present in the sulfoxide state) was obtained, which is in close agreement with the predicted N terminus of the HycD protein (Met–Ser–Val–Leu–Tyr). Thus, the larger complex consists of the predicted membrane domain of FHL (HycC plus HycD) together with the core soluble domain.

To test the hypothesis that the 250-kDa complex is comprised of a membrane-extrinsic core complex, the IMAC and SEC separation procedures were repeated using buffers lacking detergent after the initial detergent-containing cell breakage step. In this case, a single protein species was obtained with an approximate molecular mass of 250 kDa (Fig. 4*C*). No higher-molecular-weight shoulder was present, and analysis of the protein fractions by SDS-PAGE revealed the presence of only the five subunits of the core complex: FdhF, $HycE^{His}$, HycB, HycF, and HycG (Fig. 4*D*). Thus, in the absence of detergent in the chromatography steps, only the soluble core pentamer, dissociated from the membrane domain, was isolated.

Characterization of Hyd-3 Activity by PFE. Cyclic voltammetry experiments carried out under varying concentrations of H_2 immediately reveal striking features of the Hyd-3 enzyme (Fig. 5). Only a very limited change in reductive current is observed with increasing H_2 concentration. Other [NiFe] hydrogenases characterized to date exhibit significant product inhibition under such high concentrations of H_2. The experiments in Fig. 6 serve to quantify these differences. The apparent product inhibition constant for H_2 production, $K_{i,app}^{H_2}$, is 1.48 mM at pH 6, 37 °C, and −558 mV vs. Standard Hydrogen Electrode (SHE), corresponding to roughly 1.5 bar hydrogen. This simple measurement offers a clear demonstration of the unique properties of Hyd-3 among previously characterized hydrogenases (Fig. 6*C*). Whereas all previously characterized [NiFe] hydrogenases are strongly product inhibited, Hyd-3 shows a high tolerance to product inhibition, with a $K_{i,app}^{H_2}$ that is an order of magnitude greater than values for other [NiFe] hydrogenases, but is comparable to those measured previously for [FeFe] hydrogenases. The Michaelis–Menten constant for H_2 oxidation, $K_M^{H_2}$, is 34 μM at pH 6, 37 °C, and −107 mV vs. SHE. Given that both $K_{i,app}^{H_2}$ and $K_M^{H_2}$ are dependent upon the strength of H_2 binding, it is surprising that Hyd-3 is more closely comparable with other [NiFe] than with [FeFe] hydrogenases in terms of the $K_M^{H_2}$. This may be due to a higher k_{cat} for the [FeFe] enzymes relative to [NiFe] enzymes (because, for a given dissociation constant K_D for a substrate, increasing the k_{cat} has the effect of increasing K_M).

Carbon monoxide is a classic competitive inhibitor of hydrogenase activity. For hydrogenases studied to date, the sensitivity to inhibition by CO shows a strong correlation with other enzyme properties; for example, [NiFe] hydrogenases tend to be more resistant to inhibition by CO than [FeFe] hydrogenases (26), and among the [NiFe] hydrogenases, those showing a higher resistance to inhibition by CO also tend to be resistant to inhibition by O_2 (termed O_2-tolerant) (27–29). The inhibition constant of Hyd-3 for CO was assessed by chronoamperometry during H_2 oxidation and H_2 production. The K_i^{CO/H_2} is 8.2 ± 1.8 μM (at pH 6.0, 37 °C, 10% H_2 in Ar, −0.087 V vs. SHE) and the $K_{i,app}^{CO/H^+}$ during H^+ reduction is 56 ± 17 μM (at pH 6.0, 37 °C, 100% Ar, −0.537 V vs. SHE). The experimental data are shown in Fig. 7. Thus, Hyd-3 is much more tolerant to inhibition by CO than [FeFe] hydrogenases or "standard," O_2-sensitive [NiFe] hydrogenases, which tend to have K_i values in the low micromolar range. The relatively high K_i^{CO/H_2} value is nearer to that seen for the O_2-tolerant Hyd-1 from *E. coli* (26, 28).

Discussion

The disproportionation of formate to CO_2 and H_2, observed over 100 years ago as the first example of a fundamental conversion of microbial metabolism, has until now been observable only in whole cells and crude cell lysate. By using molecular genetic techniques to produce affinity-tagged FHL proteins encoded at the native chromosomal locus, and maintaining gene expression at native levels, an active, intact formate hydrogenlyase complex was purified from *E. coli*. This represents a step forward in understanding the Group 4 hydrogenases, a class that is poorly characterized to date and unique among the [NiFe] hydrogenases in containing mostly enzymes whose physiological role is H_2 production. The complex can be extracted in two forms: (*i*) a five-component complex containing HycBEFG and variable amounts of FdhF and (*ii*) an apparent seven-component complex containing HycBCDEFG and variable amounts of FdhF. The loose attachment of the formate dehydrogenase component has been previously observed (2). In this study, however, the predicted Fe–S cluster containing subunits HycB, HycF, and HycG remained tightly associated with the membranes following cell breakage (Fig. 2), suggesting further fragmentation of FHL only occurs after membrane dispersal. By analogy to Complex I, membrane attachment of HycBEFG is likely to be mediated by the HycCD proteins (Fig. 1). The putative seven-subunit complex containing HycCD was only identified in detergent-treated samples (Fig. 4*A*); however, it should be considered that HycCD has completely detached in this preparation and is behaving as a separate 575-kDa entity that overlaps the profile of the 250-kDa HycBEFG (FdhF) complex (Fig. 4). However, given that the HycCD proteins are still present following IMAC directed by just one tagged protein (HycE), this is indicative that the complete complex can maintain structural integrity at least in the early stages of this purification protocol. The predicted combined mass of HycB (21,873 Da), HycE (61,149 Da), HycF (20,309 Da), and HycG (27,999 Da) is 131.3 kDa, which perhaps points to dimerization of these proteins within a larger complex. However, the variable attachment of FdhF (itself 80 kDa) to the complex makes interpretation of SEC data challenging. The preparations described here contained no detectable HycH or HycI proteins, which are also encoded within the *hyc* operon (Fig. 1). This is consistent with these proteins having roles in the biosynthesis of FHL, rather than being constituent parts of the enzyme complex (13).

Biochemistry of Hyd-3. It is clear from the PFE experiments performed here that Hyd-3 is unique among [NiFe] hydrogenases studied to date and more closely resembles [FeFe] hydrogenases in terms of its resistance to inhibition by H_2. This should make Hyd-3 especially well suited to biotechnological H_2 production, as it would allow for accumulation of significant concentrations of H_2. The relatively low $K_M^{H_2}$ value during H_2 oxidation was somewhat unexpected, however. In general, values of $K_{i,app}^{H_2}$ and $K_M^{H_2}$ for H_2 production and oxidation, respectively, are correlated through their dependence on the strength of H_2 binding. Despite possessing a drastically increased $K_i^{H_2}$, roughly ten times the value for O_2-sensitive and a hundred times the value for O_2-tolerant enzymes (28, 30), Hyd-3 shows a $K_M^{H_2}$ value of 34 μM, only twice that of Hyd-2 from *E. coli.* In comparison, the [FeFe] hydrogenases exhibit $K_M^{H_2}$ values an order of magnitude greater (190 μM and 460 μM for *Cr*HydA1 and *Ca*HydA, respectively) (30). The value of $K_M^{H_2}$ for Hyd-3 indicates that under appropriate thermodynamic conditions, Hyd-3 would be competitive with Hyd-2 and, to a lesser extent, Hyd-1 of *E. coli*, for H_2 oxidation. The reversible nature of Hyd-3 when studied by assaying cell extracts with redox dyes is well documented (5); however, in the true physiological context, it is interesting to note that early whole-cell experiments with *E. coli* have indeed shown that exposure to high concentrations of CO_2 and H_2 resulted in the production of formate (9).

For the purpose of this study, results have been reported that were obtained with a preparation in which bidirectional activity was observed, because that should be more reflective of the known physiological activity of the complex. However, it should be noted that the catalytic waveshape seen during PFE experiments of Hyd-3 varied significantly between different batches of purified enzyme, with some batches exhibiting a large overpotential requirement for H_2 oxidation and very little H_2 production activity (Fig. S2). A recent study examining the overpotential requirement and catalytic bias of the O_2-tolerant Hyd-1 suggests that limitations on interfacial electron transfer at low potential are likely responsible for the overpotential requirement and bias for that enzyme (31). In the context of the highly labile nature of the FHL complex, it is possible that complexes with different subunit and/or cofactor composition when adsorbed at the electrode will exhibit marked differences in interfacial electron transfer. Indeed, unlike the uptake hydrogenases, which have evolved for electron transfer to the quinone pool or other external electron carriers, the FHL complex is a closed system that contains buried active sites of both an oxidase and a reductase; thus, any electron transfer into or out of the complex in vivo would lead to inefficiency. This may contribute to poor interfacial electron transfer kinetics in PFE studies. It therefore seems likely that the inconsistency observed in the catalytic bias and overpotential requirement for Hyd-3 as observed by PFE is due to the lability of the complex, which may result in slightly different variants of the complex establishing electrochemical "communication" with the electrode, some of which show inefficient electron transfer.

Fundamentally, it seems that all [NiFe] hydrogenase active sites are good bidirectional catalysts, whose activity in vivo is tuned by the properties of the associated Fe–S clusters within any specific enzyme. The result that Hyd-3 is a good H_2 producer even under high concentrations of H_2 is informative about an important difference between the active site of this enzyme and others.

The Physiological Role of FHL. Through this and previous work, including comparisons with Complex I (Fig. 1), which has recently been further structurally characterized (4, 32), it is clear that the FHL complex is membrane bound, leading to renewed suggestions that FHL enzymes could pump protons and so contribute to the transmembrane protonmotive force (33). In support of this, *Thermococcus onnurineus*, an organism producing several proteins sharing identity with *E. coli* FHL components, has been shown to be able to sustain growth with formate as the energy source (33). Since *E. coli* cannot grow with formate as the sole carbon source (34), in part because *E. coli* cannot fix CO_2 in the classical sense, understanding the physiological role of FHL in this model organism has been fraught with difficulties. However, it is possible to link FHL activity with central energy metabolism, for example *E. coli* cells treated with dicyclohexylcarbodiimide (DCCD, a nonspecific Asp crosslinker often used to inhibit F_1F_o ATP synthase) are abolished for gas production (35), although it should be noted that DCCD probably also inhibits FdhF directly because in vitro benzyl viologen dye-linked formate dehydrogenase activity was significantly reduced upon exposure of extracts to this compound (36). However, genetic evidence from both *E. coli* and *Salmonella* work show that defects in F_1F_o ATPase also abolish fermentative gas production (36, 37), adding to the hypothesis that there is chemiosmotic coupling of FHL to ATP synthesis. Indeed, experiments using uncoupling agents in *E. coli* whole cells and inverted membrane vesicles were able to give an indication that FHL could contribute to the generation of a membrane potential (38).

During the early stages of mixed acid fermentation, *E. coli* produces and secretes formate as a waste product, and only in the latter stages of a closed batch fermentation, where the formate is allowed to accumulate in the growth medium, is this formate reimported into the cell, at which point expression of the formate regulon, including FHL, is induced (14). If the FHL reaction is indeed coupled to the generation of a proton-motive force, it is perhaps difficult to reconcile why *E. coli* does not use the formate immediately upon its production. It should be noted, however, that the very small standard potential for the reaction means that the driving force, and even the spontaneity of formate disproportionation, are dependent upon the environmental conditions. Toward the end of batch fermentation, the formate concentration is relatively high and the pH is relatively low. Both of these factors act to increase the available driving force for the FHL reaction by about 30 mV per order of magnitude change. Thus, formate is disproportionated when conditions have changed in favor of increasing the free energy of the reaction. In addition, it is also important to remember that the transmembrane electrochemical gradient is lower in late- than in early-stage fermentation (39); thus, the reaction free energy required to power proton translocation would be lower at this time. Indeed, the genetics beautifully complement the chemistry in this system, because the genes encoding the FHL complex are not expressed until the environmental conditions are correct for the reaction to take place (14).

FHL is reversible (9), but the physiological relevance of fixing CO_2 to formate by modern-day *E. coli* is not clear. This activity could be an echo of the past, because a chemiosmotic model of the evolution of early life (40) suggests that an ancient organism expressing an FHL-type complex could have harnessed H_2 and CO_2 available at hydrothermal vents to reduce CO_2 to formate, which could have been used to synthesize pyruvate long before glycolytic pathways had evolved (41).

Concluding Remarks

The ability of a fast-growing, nonpathogenic, genetically amenable, model bacterium to produce H_2 gas during fermentation has always been regarded as having great biotechnological potential, especially in bioenergy research. The final barrier to progress has been the lack of detailed knowledge on the structure and function of the intact formate hydrogenlyase enzyme that is responsible for gas production, a problem exacerbated by the extremely labile nature of this large membrane-bound complex. The work outlined in this paper goes some way to addressing that problem, and paves the way for future engineering of catalysts and synthetic enzymes. Fundamentally, the work here represents,

to our knowledge, the first electrochemical characterization of a Group 4 [NiFe] hydrogenase, and it is plausible that the properties described here are common to this class of H_2-producing enzymes.

Methods

Bacterial Strains. The parental *E. coli* K-12 strain used in this study was MG1655 (F^-, λ^-, *ilvG*$^-$, *rfb-50*, *rph-1*) (42). Strain MG059b carries an engineered *hycB*^{His} allele at the native *hyc* locus. A 500-bp DNA fragment covering the *hycB* 3′ region (minus stop codon) was amplified and cloned into pFAT210 (43). Next, a 500-bp fragment covering the downstream *hycC* gene (including Shine–Dalgarno sequence and start codon for *hycC*) was amplified and cloned into the pFAT210 downstream of the *hycB*^{His} fragment. The complete *hycB*^{His} allele was then transferred to pMAK705 (44) and moved onto the *hyc* locus of MG1655 (44) to give strain MG059b. Strains MG059f (as MG1655, *hycF*^{His}) and MG059g (as MG1655, *hycG*^{His}) were prepared in a similar fashion to MG059b.

Strain MG059e1 produces a modified HycE protein bearing an internal deca-His–Gly–Ser sequence between amino acids Gly-83 and Thr-84. First, a 500-bp DNA fragment upstream and including the *hycE* Gly-83 codon was amplified by PCR using a primer encoding an extra 10 histidine codons (as well as glycine and serine codons from an engineered BamHI site) in-frame with the *hycE* sequence to codon Gly-83. The PCR product was digested with EcoRI and BamHI. Next, a 500-bp fragment downstream of, including, and in-frame with the *hycE* Thr-84 codon was amplified by PCR and digested with BamHI and XbaI. A three-way ligation was then performed involving the two PCR products and pBluescript vector that had been predigested with EcoRI and XbaI. The resultant *hycE*^{His} allele was then moved onto pMAK705 and then onto the chromosome of MG1655 to give strain MG059e1.

All plasmids and strains generated by PCR were sequenced on both strands to ensure no errors had been introduced.

Cell Fractionation and Protein Analytical Methods. For biochemical studies, *E. coli* strains were cultured under anaerobic conditions for 12–16 h at 37 °C in static, loosely stoppered 500-mL Duran bottles filled to the top with LB media supplemented with 0.4% (wt/vol) glucose to induce fermentative growth. Cells were harvested by centrifugation and washed twice in ice-cold 50 mM Tris·HCl (pH 7.4) before being suspended in the same buffer at 1 g cells per 10 mL buffer. If required, cells were lysed by sonication or French press (8,000 psi) in the presence of 10 μg/mL DNase I and 50 μg/mL lysozyme before unbroken cells and debris were removed by centrifugation resulting in a "crude extract." Total membranes were recovered by ultracentrifugation, and the membrane pellet was resuspended in an equivalent volume of 50 mM Tris·HCl (pH 7.5). A sample of the supernatant from the ultracentrifugation step was retained as the soluble protein fraction.

Protein samples were separated by SDS-PAGE by the method of Laemmli (45) and, if necessary, transferred to nitrocellulose as described (46). Protein was visualized in-gel using Instant Blue stain (Expedeon), and Western immunoblots were developed using Qiagen penta-His or NEB maltose binding protein monoclonal antibodies or in-house rabbit polyclonal antisera to the small subunit of hydrogenase-2, HybO. Tryptic peptide mass fingerprinting was performed as a service by Fingerprints Proteomics Facility, College of Life Sciences, University of Dundee. Direct protein sequencing by Edman degradation was performed as a service by Alta Biosciences, University of Birmingham.

Protein Purification. All bacterial strains tested produce histidine-tagged FHL components at natural levels under native regulatory control. For each strain, starter cultures (2 × 5 mL) were grown aerobically overnight at 37 °C in LB medium and used in their entirety to inoculate a 5L Duran filled to the top with LB supplemented with 0.4% (wt/vol) D-glucose. This anaerobic culture contained a sterile gas release system in the cap and was incubated statically at 37 °C for 16 h before the cells were harvested by centrifugation and either used immediately or flash-frozen in liquid nitrogen and stored at −80 °C.

Cell pellets (typically 6 g wet weight for each 5 L culture) were suspended by homogenizing in 50 mL B-PER (Invitrogen) bacterial cell lysis mixture that had been supplemented with 50 mM imidazole, a protease inhibitor mixture (Calbiochem), 10 μg/mL DNase I, and 50 μg/mL lysozyme. The suspension was mixed for 20 min at room temperature before unbroken cells and debris were removed by centrifugation. The resultant crude extract was loaded directly onto a 5-mL HisTrap HP column (GE Healthcare) that had been equilibrated in 20 mM Tris·HCl (pH 7.5), 200 mM NaCl, 50 mM imidazole, 0.02% (wt/vol) (DDM). Bound proteins were eluted with a 30-mL linear gradient of the same buffer containing 1 M imidazole. A single protein peak was eluted from the column, pooled, and concentrated in a Vivaspin (Millipore Inc.) filtration device (50-kDa molecular weight cutoff) and applied to a Superdex 200 10/30 size exclusion column (GE Healthcare) equilibrated in 20 mM Tris·HCl, 200 mM NaCl, 0.02% DDM. Samples prepared for GC, PFE, and TXRF experiments (Figs. 3 and 5–7) were isolated in a similar manner, except that cell lysis was carried out using a high-pressure disruptor (Constant Systems Ltd.), membranes were solubilized by addition of 0.18 g Triton X-100 (Fisher) per liter original culture medium, and column buffers contained 350 mM NaCl and 0.03% (vol/vol) Triton X-100 in place of DDM, with a final buffer exchange step into DDM-containing buffer.

Enzyme Assays. Formate-dependent hydrogen evolution (formate hydrogenlyase activity) in intact cells was assayed using a hydrogen-sensing electrode as previously described (5, 47). FHL activity of purified enzyme was detected by monitoring H_2 levels in the headspace above enzyme exposed to 50 mM potassium formate (Sigma Aldrich) at pH 6 and 25 °C using a 7890A gas chromatography system (Agilent Technologies) equipped with a Shin-Carbon ST micropacked column (Restek Corporation) and thermal conductivity detector, with N_2 as carrier gas and CH_4 as internal standard. Peak areas were analyzed using ImageJ software (US National Institutes of Health).

PFE. PFE experiments were carried out as described previously (48) except that the working electrode used was a pyrolytic graphite surface, with an area of ∼4 mm^2, bearing noncovalently attached multiwalled carbon nanotubes (MWNT). The MWNT, obtained from Sigma, were >90% carbon (trace metal basis) produced by catalytic chemical vapor deposition (outer diameter 10–15 nm, inner diameter 2–6 nm, length 0.1–10 μm). A 1 mg/mL solution of MWNT in DMF was dispersed by sonication for 15 min before pipetting onto the surface of a sanded, rinsed, and sonicated PGE electrode. The electrode was left to dry for a minimum of 2 h and was then rinsed with distilled H_2O before soaking in a 500 μg/mL solution of purified FHL containing 4 mg/mL polymixin B sulfate (Fluka) as coadsorbate.

Metal Determination. Metal analysis by ICP-MS was performed as a service by the School of Chemistry, University of Edinburgh. TXRF analysis was carried out on a PicoFox spectrometer (Bruker) as previously described (49, 50). A gallium elemental concentration standard (Sigma) was added to the protein solutions (1:1 vol/vol) before the measurements.

ACKNOWLEDGMENTS. We thank John R. Guest (Sheffield), Gary Sawers (Halle), Conny Pinske (Dundee), and Maxie Roessler (Queen Mary) for useful discussions and suggestions. This work was funded by the Biological and Biotechnological Sciences Research Council [Grants BB/H001190/1 and BB/I02008X/1 (to F.S.) and BB/H003878-1 and BB/I022309-1 (to F.A.A.)]. M.H. thanks the Deutsche Forschungsgemeinschaft (Grants Ha3265/2-1, Ha3265/3-1, and Ha3265/6-1) and the Bundesministerium für Bildung und Wissenschaft (Grant 05K14KE1) for financial support. B.J.M. acknowledges the Clarendon Fund Scholarship and Canadian Natural Sciences and Engineering Research Council for funding. F.A.A. and T.P. are Royal Society-Wolfson Research Merit Award holders.

1. Richardson DJ (2000) Bacterial respiration: A flexible process for a changing environment. *Microbiology* 146(Pt 3):551–571.
2. Sawers G (1994) The hydrogenases and formate dehydrogenases of *Escherichia coli*. *Antonie van Leeuwenhoek* 66(1-3):57–88.
3. Andrews SC, et al. (1997) A 12-cistron *Escherichia coli* operon (*hyf*) encoding a putative proton-translocating formate hydrogenlyase system. *Microbiology* 143(Pt 11):3633–3647.
4. Efremov RG, Sazanov LA (2012) The coupling mechanism of respiratory complex I —A structural and evolutionary perspective. *Biochim Biophys Acta* 1817(10):1785–1795.
5. Sawers RG, Ballantine SP, Boxer DH (1985) Differential expression of hydrogenase isoenzymes in *Escherichia coli* K-12: Evidence for a third isoenzyme. *J Bacteriol* 164(3): 1324–1331.
6. Redwood MD, Mikheenko IP, Sargent F, Macaskie LE (2008) Dissecting the roles of *Escherichia coli* hydrogenases in biohydrogen production. *FEMS Microbiol Lett* 278(1): 48–55.
7. Pakes WCC, Jollyman WH (1901) The collection and examination of the gases produced by bacteria from certain media. *J Chem Soc* 79:322–329.
8. Stephenson M, Stickland LH (1932) Hydrogenlyases: Bacterial enzymes liberating molecular hydrogen. *Biochem J* 26(3):712–724.
9. Woods DD (1936) Hydrogenlyases: The synthesis of formic acid by bacteria. *Biochem J* 30(3):515–527.
10. Böhm R, Sauter M, Böck A (1990) Nucleotide sequence and expression of an operon in *Escherichia coli* coding for formate hydrogenlyase components. *Mol Microbiol* 4(2): 231–243.
11. Sauter M, Böhm R, Böck A (1992) Mutational analysis of the operon (*hyc*) determining hydrogenase 3 formation in *Escherichia coli*. *Mol Microbiol* 6(11):1523–1532.
12. Boyington JC, Gladyshev VN, Khangulov SV, Stadtman TC, Sun PD (1997) Crystal structure of formate dehydrogenase H: Catalysis involving Mo, molybdopterin, selenocysteine, and an Fe_4S_4 cluster. *Science* 275(5304):1305–1308.

13. Rossmann R, Maier T, Lottspeich F, Böck A (1995) Characterisation of a protease from *Escherichia coli* involved in hydrogenase maturation. *Eur J Biochem* 227(1-2):545–550.
14. Rossmann R, Sawers G, Böck A (1991) Mechanism of regulation of the formate-hydrogenlyase pathway by oxygen, nitrate, and pH: Definition of the formate regulon. *Mol Microbiol* 5(11):2807–2814.
15. Maeda T, Sanchez-Torres V, Wood TK (2007) Enhanced hydrogen production from glucose by metabolically engineered *Escherichia coli*. *Appl Microbiol Biotechnol* 77(4): 879–890.
16. Thauer RK, Jungermann K, Decker K (1977) Energy conservation in chemotrophic anaerobic bacteria. *Bacteriol Rev* 41(1):100–180.
17. Raaijmakers HC, Romão MJ (2006) Formate-reduced *E. coli* formate dehydrogenase H: The reinterpretation of the crystal structure suggests a new reaction mechanism. *J Biol Inorg Chem* 11(7):849–854.
18. George GN, et al. (1998) X-ray absorption spectroscopy of the molybdenum site of *Escherichia coli* formate dehydrogenase. *J Am Chem Soc* 120(6):1267–1273.
19. Khangulov SV, Gladyshev VN, Dismukes GC, Stadtman TC (1998) Selenium-containing formate dehydrogenase H from *Escherichia coli*: A molybdopterin enzyme that catalyzes formate oxidation without oxygen transfer. *Biochemistry* 37(10):3518–3528.
20. Gladyshev VN, et al. (1996) Characterization of crystalline formate dehydrogenase H from *Escherichia coli*. Stabilization, EPR spectroscopy, and preliminary crystallographic analysis. *J Biol Chem* 271(14):8095–8100.
21. Fontecilla-Camps JC, Volbeda A, Cavazza C, Nicolet Y (2007) Structure/function relationships of [NiFe]- and [FeFe]-hydrogenases. *Chem Rev* 107(10):4273–4303.
22. Vignais PM, Billoud B (2007) Occurrence, classification, and biological function of hydrogenases: An overview. *Chem Rev* 107(10):4206–4272.
23. Vignais PM, Colbeau A (2004) Molecular biology of microbial hydrogenases. *Curr Issues Mol Biol* 6(2):159–188.
24. Vignais PM, Billoud B, Meyer J (2001) Classification and phylogeny of hydrogenases. *FEMS Microbiol Rev* 25(4):455–501.
25. Rossmann R, Sauter M, Lottspeich F, Böck A (1994) Maturation of the large subunit (HYCE) of *Escherichia coli* hydrogenase 3 requires nickel incorporation followed by C-terminal processing at Arg537. *Eur J Biochem* 220(2):377–384.
26. Goldet G, et al. (2009) Electrochemical kinetic investigations of the reactions of [FeFe]-hydrogenases with carbon monoxide and oxygen: Comparing the importance of gas tunnels and active-site electronic/redox effects. *J Am Chem Soc* 131(41):14979–14989.
27. Vincent KA, et al. (2005) Electrocatalytic hydrogen oxidation by an enzyme at high carbon monoxide or oxygen levels. *Proc Natl Acad Sci USA* 102(47):16951–16954.
28. Lukey MJ, et al. (2010) How *Escherichia coli* is equipped to oxidize hydrogen under different redox conditions. *J Biol Chem* 285(6):3928–3938.
29. Pandelia ME, Infossi P, Giudici-Orticoni MT, Lubitz W (2010) The oxygen-tolerant hydrogenase I from *Aquifex aeolicus* weakly interacts with carbon monoxide: An electrochemical and time-resolved FTIR study. *Biochemistry* 49(41):8873–8881.
30. Goldet G (2009) Electrochemical investigations of H_2-producing enzymes. D. Phil. (University of Oxford, Oxford).
31. Murphy BJ, Sargent F, Armstrong FA (2014) Transforming an oxygen-tolerant [NiFe] uptake hydrogenase into a proficient, reversible hydrogen producer. *Energy Env Sci* 7(4):1426–1433.
32. Baradaran R, Berrisford JM, Minhas GS, Sazanov LA (2013) Crystal structure of the entire respiratory complex I. *Nature* 494(7438):443–448.
33. Kim YJ, et al. (2010) Formate-driven growth coupled with H_2 production. *Nature* 467(7313):352–355.
34. Sauter M (1992) Der Formiat-Hydrogenlyase-Komplex von *Escherichia coli*: Untersuchungen zu Struktur und Funktion. PhD. (Ludwigs-Maximilians University, Munich).
35. Bagramyan KA, Martirosov SM (1989) Formation of an ion transport supercomplex in *Escherichia coli*. An experimental model of direct transduction of energy. *FEBS Lett* 246(1-2):149–152.
36. Sasahara KC, Heinzinger NK, Barrett EL (1997) Hydrogen sulfide production and fermentative gas production by *Salmonella typhimurium* require F_oF_1 ATP synthase activity. *J Bacteriol* 179(21):6736–6740.
37. Trchounian A, Bagramyan K, Poladian A (1997) Formate hydrogenlyase is needed for proton-potassium exchange through the F_oF_1-ATPase and the TrkA system in anaerobically grown and glycolysing *Escherichia coli*. *Curr Microbiol* 35(4):201–206.
38. Hakobyan M, Sargsyan H, Bagramyan K (2005) Proton translocation coupled to formate oxidation in anaerobically grown fermenting *Escherichia coli*. *Biophys Chem* 115(1):55–61.
39. Bot CT, Prodan C (2010) Quantifying the membrane potential during *E. coli* growth stages. *Biophys Chem* 146(2-3):133–137.
40. Lane N, Allen JF, Martin W (2010) How did LUCA make a living? Chemiosmosis in the origin of life. *BioEssays* 32(4):271–280.
41. Potter S, Fothergill-Gilmore LA (1993) Molecular evolution: The origin of glycolysis. *Biochem Educ* 21(1):45–48.
42. Blattner FR, et al. (1997) The complete genome sequence of *Escherichia coli* K-12. *Science* 277(5331):1453–1462.
43. Dubini A, Pye RL, Jack RL, Palmer T, Sargent F (2002) How bacteria get energy from hydrogen: A genetic analysis of periplasmic hydrogen oxidation in *Escherichia coli*. *Int J Hydrogen Energy* 27(11-12):1413–1420.
44. Hamilton CM, Aldea M, Washburn BK, Babitzke P, Kushner SR (1989) New method for generating deletions and gene replacements in *Escherichia coli*. *J Bacteriol* 171(9): 4617–4622.
45. Laemmli UK (1970) Cleavage of structural proteins during the assembly of the head of bacteriophage T4. *Nature* 227(5259):680–685.
46. Towbin H, Staehelin T, Gordon J (1979) Electrophoretic transfer of proteins from polyacrylamide gels to nitrocellulose sheets: Procedure and some applications. *Proc Natl Acad Sci USA* 76(9):4350–4354.
47. Sargent F, Stanley NR, Berks BC, Palmer T (1999) Sec-independent protein translocation in *Escherichia coli*. A distinct and pivotal role for the TatB protein. *J Biol Chem* 274(51):36073–36082.
48. Armstrong FA (2009) Dynamic electrochemical experiments on hydrogenases. *Photosynth Res* 102(2-3):541–550.
49. Reschke S, et al. (2013) Identification of a bis-molybdopterin intermediate in molybdenum cofactor biosynthesis in *Escherichia coli*. *J Biol Chem* 288(41):29736–29745.
50. Fritsch J, et al. (2011) [NiFe] and [FeS] cofactors in the membrane-bound hydrogenase of *Ralstonia eutropha* investigated by X-ray absorption spectroscopy: Insights into $O(_2)$-tolerant $H(_2)$ cleavage. *Biochemistry* 50(26):5858–5869.